EUROfusion

EUROFUSION WPJET1-CP(16) 15209

C Angioni et al.

Progress in the theoretical description and the experimental characterization of tungsten transport in tokamaks

Preprint of Paper to be submitted for publication in
Proceedings of 26th IAEA Fusion Energy Conference

This work has been carried out within the framework of the EUROfusion Consortium and has received funding from the Euratom research and training programme 2014-2018 under grant agreement No 633053. The views and opinions expressed herein do not necessarily reflect those of the European Commission.

This document is intended for publication in the open literature. It is made available on the clear understanding that it may not be further circulated and extracts or references may not be published prior to publication of the original when applicable, or without the consent of the Publications Officer, EUROfusion Programme Management Unit, Culham Science Centre, Abingdon, Oxon, OX14 3DB, UK or e-mail Publications.Officer@euro-fusion.org

Enquiries about Copyright and reproduction should be addressed to the Publications Officer, EUROfusion Programme Management Unit, Culham Science Centre, Abingdon, Oxon, OX14 3DB, UK or e-mail Publications.Officer@euro-fusion.org

The contents of this preprint and all other EUROfusion Preprints, Reports and Conference Papers are available to view online free at http://www.euro-fusionscipub.org. This site has full search facilities and e-mail alert options. In the JET specific papers the diagrams contained within the PDFs on this site are hyperlinked

Progress in the theoretical description and the experimental characterization of tungsten transport in tokamaks

C. Angioni[1], R. Bilato[1], V. Bobkov[1], A. Loarte[2], R. Ochoukov[1], T. Odstrcil[1], T. Pütterich[1], M. Sertoli[1], J. Stober[1], E. A. Belli[3], F. J. Casson[4], E. Fable[1], P. Mantica[5], M. Valisa[6], the ASDEX Upprade Team and JET Contributors*[8]

[1]Max-Planck Institut für Plasmaphysik, IPP–Euratom Association, D-85748 Garching bei München, Germany
[2]ITER Organization, Route de Vinon-sur-Verdon, CS 90 046, 13067 St Paul Lez Durance Cedex, France
[3]General Atomics, PO Box 85608, San Diego, California 92186-5608, USA
[4]CCFE, Culham Science Centre, Abingdon, OX14 3DB, UK
[5]Istituto di Fisica del Plasma, CNR/ENEA, Milano, Italy
[6]Consorzio RFX-CNR/ENEA, I-35127 Padova, Italy
[8]EUROfusion Consortium, JET, Culham Science Centre, Abingdon, OX14 3DB, UK

Corresponding Author: clemente.angioni@ipp.mpg.de

Abstract:
Recent theoretical results on the properties of turbulent transport of heavy impurities are briefly reviewed. The results of new experiments on ASDEX Upgrade are reported which investigate the impact of central wave heating on the avoidance of W accumulation in H-mode plasmas with dominant neutral beam injection heating. Experiments show that ion cyclotron and electron cyclotron heating have similar effects on the W behavior when similar power density profiles are produced with the two wave heating systems. The theory-based modelling of these experimental results allows the identification of important ingredients which govern the W transport in the central region in the presence of RF heating, but also reveals some limitations for fully quantitative predictions, also connected with the neglected impact of (1,1) MHD activity.

1 Introduction

Heavy impurities, like tungsten (W), are expected to play a critical role in a fusion reactor plasma. Heavy impurities are transported by both neoclassical and turbulent mechanisms. Transport models which are used to predict the W density profiles need to include an adequate level of sophistication in order to be realistic and provide a robust understanding

*See the author list of "Overview of the JET results in support to ITER" by X. Litaudon et al. to be published in Nuclear Fusion Special issue: overview and summary reports from the 26th Fusion Energy Conference (Kyoto, Japan, 17-22 October 2016)

of the mechanisms by which W accumulation can be avoided. This is required in order to assess the possibilities of controlling W accumulation in future devices. Important elements have been identified in the modelling to obtain predictions which agree with JET and ASDEX Upgrade (AUG) experimental results [1, 2, 3], in particular connected with the poloidal inhomogeneity of the W density distribution, which strongly modifies the neoclassical transport [4, 5] and also non-negligibly affects the turbulent transport [6]. The poloidal inhomogeneity of the W density is produced by centrifugal effects [1, 3] and can be also affected by the presence of auxiliary heated minority species with anisotropic temperatures [7, 2]. The most commonly applied method to avoid W accumulation is the application of central RF heating [8, 9, 10]. In this contribution we specifically address some of the open questions connected with the impact of central heating on the W behaviour. In Section 2 we review the results of a gyrokinetic study on the impact of the electron to ion heat flux ratio on the turbulent transport of the impurities. In Section 3 we present the results of a new experiment performed at AUG which compares the impact of central ECH and central ICRH on the W behaviour in a NBI heated plasma in H-mode. In section 4 the experimental results are modelled in order to shed light on the relative role of the transport mechanisms governing the W density behaviour. In Section 5 we draw some general conclusions in view of the extrapolation to future devices, starting from the results in AUG and JET.

2 Theoretical study of the impact of the electron heating fraction on turbulent impurity transport

A gyrokinetic study has been performed to elucidate how the turbulent diffusion of impurities depends on the electron to ion heat flux ratio Q_e/Q_i, keeping constant the total heat flux $Q_e + Q_i$ [11]. Nonlinear gyrokinetic simulations with GKW [12] show that the turbulent diffusion of highly charged impurities can vary by more than one order of magnitude at fixed value of the total turbulent heat flux. Maximum values of the impurity diffusion are obtained when the turbulence produces comparable levels of electron and ion heat fluxes, or the electron heat flux is slightly larger than the ion heat flux. The ratio of the impurity diffusion coefficient to the plasma effective heat conductivity can vary from minimum values below 0.4 for dominant electron and ion heat fluxes, to maximum values above 4, when Q_e/Q_i is between 1.5 and 2. This dependence is also reproduced by corresponding linear numerical calculations. An analytical treatment shows that this effect is a direct consequence of the different energy moments which produce particle and heat transport in combination with the energy and charge dependencies of the curvature and grad B drifts. Plasma conditions which maximize particle transport do not correspond to those which maximize heat transport, as they correspond to different characteristic real eigenfrequencies. This effect is significantly reinforced for highly charged impurities, as a consequence of the inverse dependence of the curvature and grad B drift frequency on the impurity charge. Thereby, turbulent states which are caused by linear instabilities with frequencies which sit between the electron and ion drift frequencies produce diffusion coefficients of highly charged impurities which are larger than the corresponding

electron, ion and effective heat conductivities. In contrast, conditions where the electron or the ion heat fluxes are largely dominant produce impurity diffusion coefficients which are significantly smaller than the heat conductivities [11]. At these intermediate turbulence conditions which produce comparable electron and ion heat fluxes, the turbulent state is often due to the combination of ITG modes and TEM which are dominant or subdominant in different parts of the linear spectrum. Nonlinear gyrokinetic simulations with GKW show that in these conditions the turbulent convection of heavy impurities is produced by the combination of the effects produced by both dominant and subdominant linear modes [13]. In conditions in which the dominant linear mode (ITG) produces a small inward convective flux whereas the subdominant linear mode (TEM) produces a large outward convection, the nonlinear convective flux turns out to be directed outward, opposite to the direction of the dominant linear mode, but consistent with a quasi–linear model which takes into account properly weighted contributions of both dominant and subdominant modes in the radial fluxes [13].

3 Experimental investigation of the W response to central ECH and ICRH

A new experiment has been performed in AUG to compare the impact of central ECH and central ICRH on W transport in otherwise similar conditions. Plasma discharges of 1 MA and magnetic field around 2.5 T ($q_{95} \simeq 4$) have been produced at the line averaged electron density of $n_e = 7.2 \;\; 10^{19} \;\; m^{-3}$, with the current flat top phase in H-mode, heated by 7.5 MW of constant NBI heating power and by decreasing power steps of central ECH and ICRH. Time traces of one of the discharges with ICRH power steps are presented in Fig. 1. With decreasing ICRH power (Fig. 1b), the W concentration at the center (Fig. 1c) (measured with high temporal resolution by the grazing incidence spectrometer (GIW)) progressively increases, eventually leading to central accumulation, as also shown by the corresponding fast increase of the total radiated power (Fig. 1a). Since the level of central localization of the ICRH power in AUG is relatively limited as compared to the possibilities of the ECH power, discharges with different power steps of ECH have been applied with 3 gyrotrons all converging to a deposition close to the magnetic axis ($\rho_{\rm dep} \simeq 0.1$) as well as with 3 gyrotrons aiming at different radial locations in order to approximatively reproduce the profile of the deposited power from ICRH (as obtained by TORIC–SSFPQL [14] simulations applied to a previous similar plasma). A comparison of the profiles of the deposited power with localized ECH, with broad ECH, (computed by TORBEAM [15]) as well as with ICRH (computed with TORIC–SSFPQL [14]) are presented in Fig. 2. In AUG, ICRH is accompanied by an additional W source as compared to ECH, which has been recently minimized by using the new 3–strap ICRF antennas [16]. Discharges with ECH power scans have been also performed with additional W sources, in order to ensure that the different source levels do not affect the core W transport analysis, which is the main goal of this study. A summary of the results obtained in a series of 6 shots is presented in Fig. 3, where the ratio of the central concentration to a peripheral concentration of W (measured by GIW) and averaged over

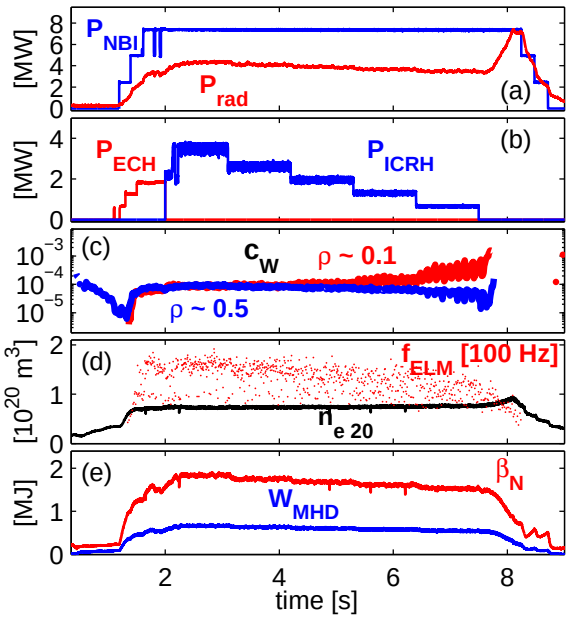

Fig. 1. Time traces of AUG shot ♯32404 with decreasing steps of ICRH power

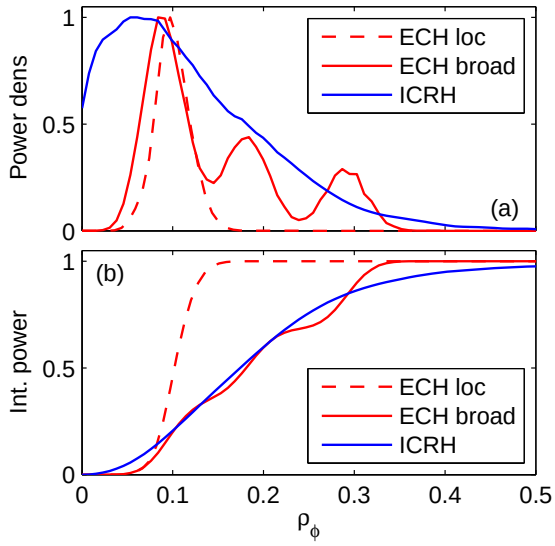

Fig. 2. Power density (a) and integrated power (b) profiles with localized and broad ECH (TORBEAM) [15] and with ICRH (TORIC-SSFPQL) [14]

the different phases of constant heating power are plotted as a function of the total RF heating power. While this plot shows a certain level of scatter, it confirms the beneficial trend of increasing RF heating power to decrease the central W concentration. The most efficient effect is clearly obtained with localized ECH, whereas broad ECH deposition has a somewhat weaker effect, comparable with that of central ICRH, which however requires significantly higher total RF powers in order to obtain flat concentrations of W in the central region. Since ICRH is delivering both electron and ion heating to the plasma, the same data points are plotted as a function of the ICRH electron heating power only, as computed by the TORIC-SSFPQL package [14], and which exhibit a trend very much consistent with that observed with ECH. A more precise description of the impact of the RF heating on the W behaviour in the core is obtained by plotting the ratio of central ($r/a = 0.05$) to the off–axis($r/a = 0.35$) flux–surface–averaged W density (reconstruced by a SXR W density diagnostic [17]) as a function of the fraction of the electron heating power absorbed inside that radial window ($r/a = 0.25$) (computed with power balance analysis by TRANSP). The results are presented in Figs. 4 and 5. In Fig. 4, points are sampled by type of heating (localized ECH, broad ECH and ICRH). We observe that different types of heating produce comparable effects (ICRH being slightly more efficient at the same fraction of electron heating power, but not at total injected RF power). The good inverse correlation found between the W peaking and the electron heating fraction with both ECH and ICRH suggests that, at least in these conditions, with a background of 7.5 MW of NBI, the increase of the electron heating fraction produced by the additional RF heating is the main cause of the flattening of the W density profile. This observation is qualitatively consistent with the theoretical result of the impact of Q_e/Q_i on the impurity turbulent diffusion, presented in Section 2. We also observe that centrally hollow W

density profiles are only obtained with the highest fractions of electron heating, achieved by localized ECH. Since MHD activity is observed to impact the shape of the W density profile in the core [18, 19], in Fig. 5 points are also sampled by type of MHD activity. We observe that localized electron heating (that is, largest values of Q_e/Q_{tot}) correlates with the presence of a slow (low frequency) 1/1 mode, in replacement or in addition to the more regular fast 1/1 mode. We find that all of the cases which develop a centrally hollow W density profile also exhibit a slow 1/1 mode, suggesting that the presence of this mode is important for the development of the central hollowness, consistent with the results of [18, 19].

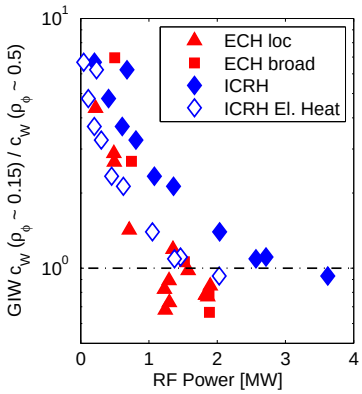

Fig. 3. Ratio of central to peripheral W concentration measured by GIW vs RF heating power

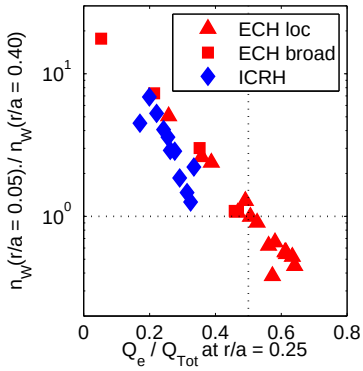

Fig. 4. Peaking factor of the W density in the core vs the electron heating fraction inside $r/a = 0.25$

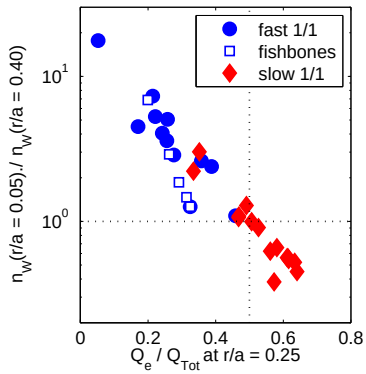

Fig. 5. Same as Fig. 4 with points sampled by type of MHD activity

4 Modelling of the experimental results

The drift–kinetic code NEO [20] and the gyro–kinetic code [12] are applied to model the experimental results, aiming to identify the ingredients which are required to reproduce the experimental trends. A representative set of 12 heating phases from the experimental database presented in Section 3 is selected, out of which 5 are with auxiliary ICRH and 7 are with auxiliary ECH. Fig. 6 shows a comparison of the neoclassical results at r/a = 0.25 obtained neglecting (open symbols) and including (full symbols) the poloidal asymmetries, plotted as a function of the experimentally applied RF heating power. Different symbols show different types of heating, as reported in the legend. For the ICRH cases, we also show results which include the poloidal asymmetry produced by centrifugal effects only, and neglect the impact of the H minority (crosses '+'). We observe that the neoclassical ratio D_W/χ_i (Fig. 6b) is strongly increased by the centrifugal effects, consistent with previous studies [1, 2, 3]. We also observe that the impact of H minority is non–negligible in the cases with highest ICRH power, leading to a reduction of the parameter D_W/χ_i, as a consequence of the reduction of the W LFS localization [4]. The inclusion of poloidal asymmetry also modifies the W convection (Fig. 6a), leading to inward convection in the majority of cases, consistent with previous analyses [4, 3], The impact of the H minority leads to a reversal of the convection from inward (negative) to outward (positive) for the cases with highest ICRH power, also consistent with previous results [4, 2].

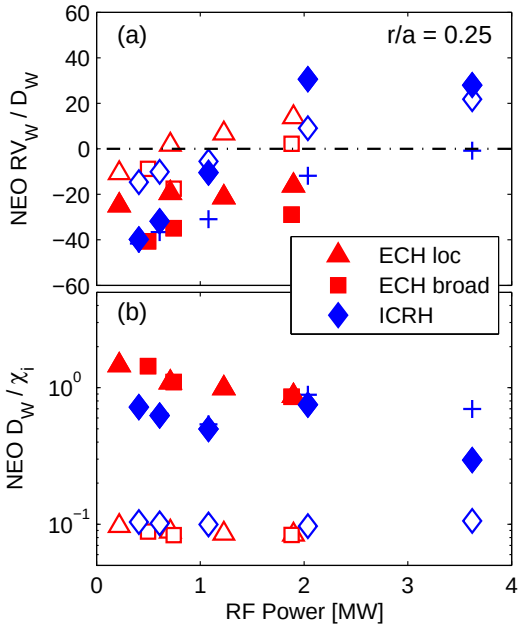

Fig. 6. Transport coefficients at $r/a = 0.25$ computed by NE0 with (full) and without (open) poloidal asymmetries of the W densities. Crosses ('+') show results with centrifugal effects only for the ICRH cases (impact of ICRH H minority is neglected).

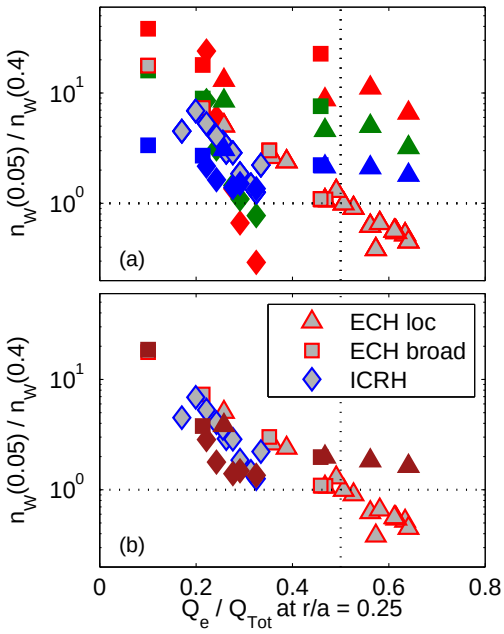

Fig. 7. Same as Fig. 4 (here experimental data are plotted with grey symbols with colored edges), compared to results from simple models (a): with $D_{turb}/\chi_{\rm eff} = 0$ (red), 0.1 (green), 1 (blue), (b): with $D_{turb}/\chi_{\rm eff}$ which fits the theoretical results of [11] as a function of Q_e/Q_i (brown).

We introduce a simplified model for W transport in the central region of the plasma, where the turbulent convection of W is neglected with respect to the neoclassical convection

$$\frac{R\Gamma_W}{n_W} = \left(D_{neo} + \frac{D_{turb}}{\chi_{\rm eff}}\chi_{\rm eff}\right)\frac{R}{L_{nW}} + V_{neo}.$$

In the framework of this model, using the neoclassical results of NEO, we test whether a constant ratio of $D_{turb}/\chi_{\rm eff}$ delivers results which are consistent with the experimental observations. Fig. 7(a) demonstrates that no choice of a constant D_{turb}/χ is consistent with all of the data from low to high electron heat fraction (shown in shadowed-colored symbols). This suggests that only a variation of the turbulent ratio D_{turb}/χ_i as a function of the electron heating fraction can explain the results, in support to the theoretical results presented in Section 2 [11]. By utilizing a polynomial fit of the theoretical results of $D_{turb}/\chi_{\rm eff}$ as a function of Q_e/Q_i [11], we obtain the results presented in Fig. 7(b), which are more consistent with the experimental trend as compared to any assumed value of constant D_{turb}/χ. When the actual turbulent transport results (computed by GKW linear runs at a single representative wave number $k_y\rho_i = 0.4$) are taken into account in the prediction of the W density, along the modelling approach described in [1, 2, 3], the results (Fig. 8) reproduce the experimental trends, although, particularly for the ECH

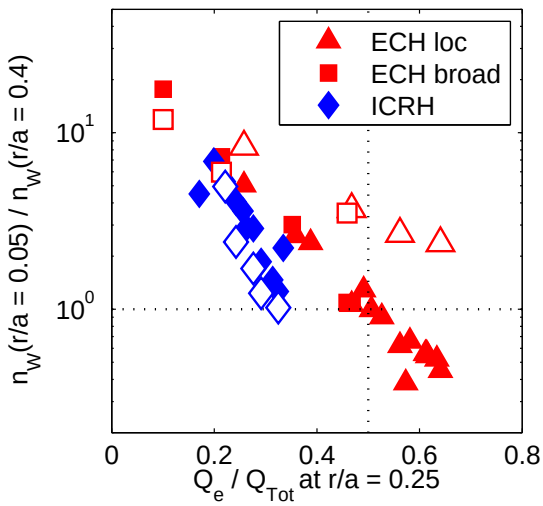

Fig. 8. Same as Fig. 4, compared with the prediction of combined NEO and GKW linear calculations (open symbols).

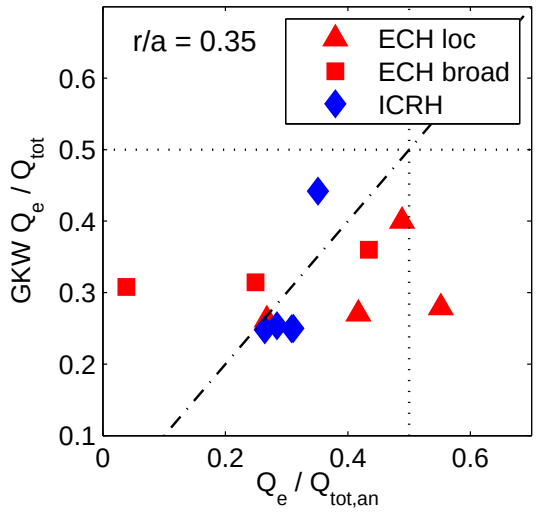

Fig. 9. Fraction of the electron heat flux predicted by linear GKW calculations compared to TRANSP power balance.

cases at high power, the central hollowness is not reproduced. The cases with ICRH are well reproduced by the modelling, where the inclusion of the H minority has a non–negligible effect. The poor level of agreement for the ECH cases with largest electron heat flux fraction reveals the most important limitations of this modelling. The results confirm that the observed central hollowness of the W density profiles in the presence of central ECH is not reproduced by transport models which assume axisymmetric equilibria and support the hypothesis of the relevance of (1,1) MHD activity [19]. An additional problem is related to the difficulty of producing turbulent transport simulations which match the experimental electron to ion heat flux ratio in the innermost region and therefore produce the correct ratio of the W diffusion to heat conductivity. The level of disagreement on the electron to ion heat flux ratio which has been obtained by these single wave number linear gyrokinetic calculations with the nominal (measured) temperature and density profiles is shown in Fig. 9. Additional linear and nonlinear simulations are being performed to investigate these aspects, as well as the potential role of subdominant modes in these experimental conditions. In addition, ETG modes are also found unstable by GKW linear calculations, and the actual fraction of electron heat flux which is produced at the large and intermediate scales which are relevant for W transport is difficult to assess quantitatively.

5 Conclusions

A gyrokinetic study shows that the ratio of the turbulent diffusivity to the heat conductvity is a sensitive function of the electron to ion heat flux ratio Q_e/Q_i and reaches maximum values when $Q_e \simeq 1.5Q_i$ [11]. In these conditions linearly unstable subdominant modes can significantly impact the turbulent convection [13]. Experiments in AUG show that central ECH and central ICRH applied to NBI heated H-mode plasmas have similar

effects on the W behaviour when they produce comparable fractions of electron heat flux. The modelling reveals that the dependence of the ratio of the diffusion to heat conduction D_W/χ on the electron to ion heat flux ratio is an important element in order to obtain the same trend as observed in these experiments. The impact of ICRH H minority is also found to be non–negligible in the modelling. The observed central hollow W density profiles in the presence of centrally localized high ECH power is not reproduced by the modelling. The central hollowness can be due to the presence of (1,1) MHD modes [18, 19], which are neglected in the modelling. These experiments in AUG, and the corresponding modelling, confirm that, in the presence of strong central electron heating, neoclassical impurity convection can be efficiently contrasted by turbulent diffusion. With increasing size of the device and increasing plasma current, and consequent increasing confinement, the achievement of higher temperatures at the same densities and the larger magnetic field lead to a reduced neoclassical transport with respect to the turbulent transport, which is favorable for the control of heavy impurity accumulation. This trend is confirmed by actual neoclassical transport calculations combined with power balance analyses of a selection of AUG and JET plasmas [13]. This suggests that the capability of offsetting the neoclassical convection by turbulent diffusion will require lower levels of central heating power per particle in devices like ITER and DEMO as compared to present devices like AUG [13].

Acknowledgments This work has been carried out within the framework of the EUROfusion Consortium and has received funding from the Euratom research and training programme 2014-2018 under grant agreement No 633053. The views and opinions expressed herein do not necessarily reflect those of the European Commission.

References

[1] Angioni C. *et al* 2014 *Nucl. Fusion* **54** 083028.
[2] Casson F. J. *et al* 2015 *Plasma Phys. Control. Fusion* **57** 014031.
[3] Angioni C. *et al* 2015 *Phys. Plasmas* **22** 055902.
[4] Angioni C, Helander P. 2014 *Plasma Phys. Control. Fusion* **56**, 124001.
[5] Belli E., Candy J., Angioni C. 2014 *Plasma Phys. Control. Fusion* **56**, 124002.
[6] Angioni C. *et al* 2012 *Phys. Plasmas* **19** 122311.
[7] Bilato R., Maj O. and Angioni C. 2014 Nucl. Fusion **54** 072003.
[8] Rice J. E. *et al* 2002 *Nucl. Fusion* **42** 510.
[9] Dux R. *et al* 2003 Plasma Phys. Control. Fusion **45** 1815.
[10] Neu R. *et al* 2003 J. Nucl. Mater. **313** 116.
[11] Angioni C. *et al* 2015 *Phys. Plasmas* **22** 120501.
[12] Peeters A. G. *et al* 2009 Comp. Phys. Commun. **180** 2650.
[13] Angioni C. *et al* 2016 Nucl. Fusion accepted for publication.
[14] Brambilla M. and Bilato R. 2009 Nucl. Fusion **49** 085004.
[15] Poli E., Peeters A.G. and Pereverzev G.V. 2001 Comp. Phys. Comm. **136** 90.
[16] Bobkov V. *et al* 2016 Nucl. Fusion **56** 084001.
[17] Sertoli M. *et al* 2015 Plasma Phys. Control. Fusion **57** 075004.
[18] Gude A. *et al* 2010 37th EPS Conf. Plasma Physics, P4.124
[19] Sertoli M. *et al* 2015 Nuclear Fusion **55** 113029.
[20] Belli E. and Candy J. 2012 Plasma Phys. Control. Fusion **54** 015015